

ANALYTICAL SOLUTION OF STRESSES IN ISOTROPIC DISC COMPOSED OF FUNCTIONALLY GRADED MATERIAL WITH VARIABLE COMPRESSIBILITY AND THICKNESS
ANALITIČKO REŠAVANJE NAPONA U IZOTROPNOM DISKU OD FUNKCIONALNOG KOMPOZITNOG MATERIJALA PROMENLJIVE STIŠLJIVOSTI I DEBLJINE

Originalni naučni rad / Original scientific paper
Rad primljen / Paper received: 26.06.2024
<https://doi.org/10.69644/ivk-2024-03-0330>

Adresa autora / Author's address:
Jaypee Institute of Information Technology, A-10, Sector 62,
Noida (Uttar Pradesh), India Pin code 201307
R. Sharma  0009-0007-2895-9626 A. Nagar  0009-0005-2696-9551 *email: richa.ggit@gmail.com

Keywords

- functionally graded materials
- piezoelectric materials
- rotating discs
- plastic theory
- transition theory
- variable thickness

Abstract

Functionally graded materials (FGMs) have numerous engineering applications due to their unique properties that vary continuously across the material structure. This study presents an analytical investigation into the stress analysis of a functionally graded disc subjected to pressure on the disc's inner surface. The considered disc is composed of a combination of two or more materials with distinct mechanical properties, exhibiting a gradual variation in composition from the centre to the outer radius. The governing differential equation is solved analytically, elastic-plastic stresses and pressure are obtained. With the help of graphs and mathematical calculations, it is perceived that variable compressibility and variable thickness have substantial impact on the performance of a functionally graded isotropic material. Disc of copper has higher circumferential stresses than steel. It can be concluded that the annular disc of functionally graded material (copper) is more suitable for engineering design than that of the disc made of steel.

INTRODUCTION

The creation of rotating discs has long been a source of intrigue in the world of engineering design, with beneficial applications including turbines, rotors, computer disc drives, and so on. The material's strength plays an essential role for all of these applications. Historically, homogenous materials were utilised to make rotating discs, but current researchers are intrigued by functionally graded materials (FGMs) due to their different mechanical properties. FGMs are advanced composite materials designed to endure extremely high temperatures and are used in technological applications such as spaceflight and aviation. Rotating functionally graded discs have several uses, including flywheels, computers, internal combustion engines, electric motors, aeronautical structures, and ship propellers.

Isotropic materials have physical features that are identical in all directions. In other words, despite the direction in which they are evaluated, their properties, such as density,

Ključne reči

- funkcionalni kompozitni materijali
- pijezelektrični materijali
- rotirajući disk
- teorija plastičnosti
- teorija prelaznih napona
- promenljiva debljina

Izvod

Funkcionalni kompozitni materijali (FGM) imaju brojne inženjerske primene zbog njihovih posebnih osobina, koje se kontinualno menjaju sa strukturom materijala. U ovom radu se analitički razmatra naponska analiza u disku od funkcionalnog kompozitnog materijala, pod dejstvom pritiska na unutrašnju površinu. Razmatrani disk je izrađen od dva ili više materijala sa specifičnim mehaničkim osobinama, u kojem se menja sastav od centra ka spoljnoj površini. Odgovarajuća diferencijalna jednačina se rešava analitički, a dobijeni su elastoplastični naponi i pritisak. Matematički proračun i grafički prikaz pokazuju da promenljiva stišljivost i promenljiva debljina imaju značajnog uticaja na svojstva funkcionalnog izotropnog kompozitnog materijala. U disku od bakra se javljaju veći cirkularni naponi u odnosu na čelični materijal. Zaključuje se da je prstenasti disk od funkcionalnog kompozitnog materijala (bakar) pogodniji za inženjersku primenu u odnosu na disk od čelika.

strength, and stiffness, are the same. This indicates that the material reacts evenly under loads and deformations, and its characteristics have no directional dependence. Metals, polymers, and ceramics are instances of isotropic materials. These materials are frequently employed in engineering applications that need consistent behaviour, such as the construction of structural parts or machine components.

Some authors use the classical theory for stress analysis, as follows: Sahni and others /1/ obtained a Frobenius series solution for a non-circulatory cylinder formed of FGM that obeys the exponential law variation in material properties across radii and found that radial stress is contractive at the cylinder's internal radii and tends towards zero at the cylinder's outer radii. To specify the fracture behaviour of piezoelectric materials, Tan et al. /2/ created a novel phase field computational framework including a temperature effect. Mehta and others /3/ discovered by stress analysis of FGM disk and demonstrated that the disc with a quadratic temperature profile rises above the disc with the linear temperature

profile. Lieu et al. /4/ developed an iso geometric Bézier FE technique for performing static bending and short examination of piezoelectric (FGP) plates reinforced with graphene platelets (GPLs). Nam and others /5/ assured that the advanced method is applicable for modelling both thick and thin structures. Sharma and Yadav /6/ obtained thermal elastic-plastic stresses and strains for rotating annular disk by making use of FDM with Von-Mises' yield criterion and nonlinear strain hardening measure. Shi and Xie /7/ evaluated the analytical solutions of stress and displacement fields of the FG cylinder under internal pressure and compared the results with existing results of related simplified problems. Kholdi and others /8/ studied the stress analysis of a rotating annular disc formed of FGMs using Successive Approximation Method (SAM). Bahaloo and Nayeb-Hashemi /9/ investigated an FG rotating disc and evaluated the stress analysis and thermoelastic instability of the disc.

Bagheri, Ayatollahi, Mousavi /10/ investigate the dynamic stress intensity parameters of multiple moving cracks with arbitrary patterns placed along the FGP strip by using a distributed dislocation approach.

Some authors employed the transition theory for stress analysis, as follows: Sharma et al. /11-16/ investigated creep stresses in transversely isotropic cylinder having thick walls formed of FGM with internal and external pressure. Sharma and Sahni /11/ applied the concept of Seth's mid-zone theory to find out the analytical solution for creep stresses in a thin, spinning disc formed of piezoelectric material that is being compressed inside. Chand, et al. /17/ evaluated the stresses in an annular isotropic disc under internal pressure and found hoop stress to be the highest near the compressible material's disc's outer surface, in contrast to incompressible material. Matvienko et al. /18/ studied plastic deformation of a rotating annular disk formed of aluminium dispersion-hardened alloys using mechanical tensile tests and a structured study using optical microscopy methods. Es-Saheb and Fouad /19/ studied creep behaviour in a rotating thick-walled cylinder of Al-SiC_p composite subjected to constant load as well as internal and external pressures, both analytically and numerically, using FEM. Godana et al. /20/ used Seth's mid-zone theory and generalised strain measure theory to model the elastoplastic deformation in a transversely isotropic spherical shell under thermal gradient and uniform pressure.

In all the above studies, elastic-plastic and creep stresses are evaluated for different structures like a thin rotating disc, a thick-walled cylinder, rectangular plates, spherical shells formed of different materials like functionally graded piezoelectric, functionally graded transversely isotropic, transversely isotropic piezoelectric, etc., under different conditions, i.e., pressure and temperature.

In the earlier study, the behaviour of stresses and pressure are attained using transition theory in an annular disc formed of homogeneous isotropic material under uniform pressure. The objective of the present study is to investigate the impact

of different parameters (i.e., compressibility and thickness) on the performance of the functionally graded isotropic disc used for designing purposes in the field of engineering. In the present problem, transitional stresses are evaluated in an annular disc formed of functionally graded isotropic material with varying compressibility and varying thickness exposed to internal pressure. The disc's compressibility and thickness are presumed to be changing from point to point in the disc.

MATHEMATICAL FORMULATIONS

Consider a thin rotating disc with inner radius r_1 and outer radius r_2 , under internal pressure p , presumed to be symmetric with reference to the mid plane, and for varying thickness the profile of isotropic rotating disc is given as:

$$h = h_0 (r/r_1)^m, \quad (1)$$

where: m is thickness parameter. The disc's angular velocity is assumed to be ω . The thin annular disc under consideration is in state of plane stress, i.e., $T_{zz} = 0$.

In polar form, displacement co-ordinates u , v , and w are presumed to be

$$u = r(1 - \beta), \quad v = 0, \quad \text{and} \quad w = dz, \quad (2)$$

where: β is a function $\beta(r)$, where $r = \sqrt{(x^2 + y^2)}$, and d is a constant.

By employing the strain measure, the strain components are given as

$$e_{rr} = \frac{1}{n} [1 - [2(r\beta' + \beta) - 1]^{n/2}], \quad e_{\theta\theta} = \frac{1}{n} [1 - (2\beta - 1)^{n/2}], \\ e_{zz} = \frac{1}{n} [1 - (1 - 2d)^{n/2}], \quad e_{r\theta} = e_{\theta z} = e_{zr} = 0, \quad (3)$$

where: n is strain measure; and $\beta' = d\beta/dr$.

These are the stress-strain relationships for this problem:

$$T_{rr} = (\lambda + 2\mu)e_{rr} + \lambda e_{\theta\theta}, \\ T_{\theta\theta} = \lambda e_{rr} + (\lambda + 2\mu)e_{\theta\theta}, \\ T_{zz} = T_{zr} = T_{r\theta} = T_{\theta z} = 0. \quad (4)$$

Substituting Eq.(3) into Eq.(4), we obtain

$$T_{rr} = \frac{(\lambda + 2\mu)}{n} [1 - [2\beta(P+1) - 1]^{n/2}] + \frac{\lambda}{n} [1 - (2\beta - 1)^{n/2}], \\ T_{\theta\theta} = \frac{\lambda}{n} [1 - [2\beta(P+1) - 1]^{n/2}] + \frac{(\lambda + 2\mu)}{n} [1 - (2\beta - 1)^{n/2}], \\ \text{where: } r\beta' = \beta P \text{ (} P \text{ is a } \beta\text{'s function; and } \beta \text{ is a function of } r\text{).} \\ \text{After substituting the values of } \lambda = 3(1 - C)/C(3 - 2C), \\ \lambda + 2\mu = 3/C(3 - 2C), \text{ and } 2\mu = 3/(3 - 2C), \text{ we obtain} \\ T_{rr} = \frac{3}{nC(3 - 2C)} [1 - [2\beta(P+1) - 1]^{n/2}] + \frac{3(1 - C)}{nC(3 - 2C)} [1 - (2\beta - 1)^{n/2}] \\ T_{\theta\theta} = \frac{3(1 - C)}{nC(3 - 2C)} [1 - [2\beta(P+1) - 1]^{n/2}] + \frac{3}{nC(3 - 2C)} \times \\ \times [1 - (2\beta - 1)^{n/2}], \quad (5)$$

where: $C = 2\mu/(\lambda + 2\mu)$ is the compressibility of the material.

For functionally graded, the compressibility of the disc is considered as $C = C_0(r/r_2)^k$, where C_0 is a constant. We have

$$T_{rr} = \frac{3}{nC_0 \left(\frac{r}{r_2}\right)^k \left(3 - 2C_0 \left(\frac{r}{r_2}\right)^k\right)} [1 - [2\beta(P+1) - 1]^{n/2}] + \frac{3 \left(1 - C_0 \left(\frac{r}{r_2}\right)^k\right)}{nC_0 \left(\frac{r}{r_2}\right)^k \left(3 - 2C_0 \left(\frac{r}{r_2}\right)^k\right)} [1 - (2\beta - 1)^{n/2}],$$

$$T_{\theta\theta} = \frac{3 \left(1 - C_0 \left(\frac{r}{r_2} \right)^k \right)}{nC_0 \left(\frac{r}{r_2} \right)^k \left(3 - 2C_0 \left(\frac{r}{r_2} \right)^k \right)} [1 - [2\beta(P+1) - 1]^{n/2}] + \frac{3}{nC_0 \left(\frac{r}{r_2} \right)^k \left(3 - 2C_0 \left(\frac{r}{r_2} \right)^k \right)} [1 - (2\beta - 1)^{n/2}]. \quad (6)$$

The rotating disc's equation of equilibrium:

$$\frac{d}{dr} (r h T_{rr}) - h T_{\theta\theta} = 0. \quad (7)$$

By putting T_{rr} and $T_{\theta\theta}$ values from Eq.(6) into Eq.(7), the regulating differential equation is attained as

$$\begin{aligned} & \left(-\frac{n}{r} \beta^2 P [2\beta(P+1) - 1]^{n/2-1} \right) \frac{dP}{d\beta} = \frac{n}{r} \beta P (P+1) [2\beta(P+1) - 1]^{n/2-1} + \left(3 - 2C_0 \left(\frac{r}{r_2} \right)^k \right)^{-1} \left(\frac{3k}{r} - \frac{4kC_0}{r_2} \left(\frac{r}{r_2} \right)^{k-1} \right) [1 - [2\beta(P+1) - 1]^{n/2}] + \\ & + \frac{k}{r} C_0 \left(\frac{r}{r_2} \right)^k [1 - (2\beta - 1)^{n/2}] + \frac{n}{r} \beta P (2\beta - 1)^{\frac{n}{2}-1} \left(1 - C_0 \left(\frac{r}{r_2} \right)^k \right) + \left(3 - 2C_0 \left(\frac{r}{r_2} \right)^k \right)^{-1} \left(1 - C_0 \left(\frac{r}{r_2} \right)^k \right) \left(\frac{3k}{r} - \frac{4kC_0}{r_2} \left(\frac{r}{r_2} \right)^{k-1} \right) [1 - (2\beta - 1)^{n/2}] + \\ & + \frac{n\alpha\theta_0}{r} \frac{1-k \log \left(\frac{r}{r_2} \right)}{\log \left(\frac{r_1}{r_2} \right)} \left(3 - 2C_0 \left(\frac{r}{r_2} \right)^k \right)^{-1} - \frac{1}{r} C_0 \left(\frac{r}{r_2} \right)^k \left((2\beta - 1)^{n/2} - (2\beta(P+1) - 1)^{n/2} \right) - \frac{m}{r} [1 - [2\beta(P+1) - 1]^{n/2}] - \\ & \frac{m}{r} \left(1 - C_0 \left(\frac{r}{r_2} \right)^k \right) [1 - (2\beta - 1)^{n/2}]. \end{aligned} \quad (8)$$

Boundary conditions that must be used at the disc's inner and outer surfaces are presumed to be

$$\begin{aligned} T_{rr} &= -p \quad \text{for } r = r_1 \\ T_{rr} &= 0 \quad \text{for } r = r_2. \end{aligned} \quad (9)$$

Conversion from elastic to plastic

According to the Seth's mid-zone theory, the conversion from elastic to plastic takes place at transformation point $P \rightarrow \pm\infty$. For estimating the stresses, R is considered as the transition function in the form of radial stress T_{rr} :

$$R = T_{rr} + B, \quad R = \frac{3 \left(1 - C_0 \left(\frac{r}{r_2} \right)^k \right)}{nC_0 \left(\frac{r}{r_2} \right)^k \left(3 - 2C_0 \left(\frac{r}{r_2} \right)^k \right)} [1 - [2\beta(P+1) - 1]^{n/2}] + \frac{3 \left(1 - C_0 \left(\frac{r}{r_2} \right)^k \right)}{nC_0 \left(\frac{r}{r_2} \right)^k \left(3 - 2C_0 \left(\frac{r}{r_2} \right)^k \right)} [1 - (2\beta - 1)^{n/2}] + B, \quad (10)$$

where: B is any constant.

Considering logarithmic differentiation of Eq.(10) w.r.t. r and putting $dP/d\beta$ value from Eq.(8) and then employing $P \rightarrow \pm\infty$ and integrating we get

$$R = A r^m e^{\frac{-C_0}{k} \left(\frac{r}{r_2} \right)^k}, \quad (11)$$

where: A is the integration constant.

Equating Eqs. (10) and (11) and by putting T_{rr} value in Eq.(7), we achieve radial and circumferential stresses as

$$T_{rr} = A r^m e^{\frac{-C_0}{k} \left(\frac{r}{r_2} \right)^k} - B, \quad T_{\theta\theta} = (m+1) \left(A r^m e^{\frac{-C_0}{k} \left(\frac{r}{r_2} \right)^k} - B \right) + A r^m e^{\frac{-C_0}{k} \left(\frac{r}{r_2} \right)^k} \left(m - C_0 \left(\frac{r}{r_2} \right)^k \right). \quad (12)$$

Using Eq.(9), we have:

$$A = \frac{-p}{r_1^m e^{\frac{-C_0}{k} \left(\frac{r_1}{r_2} \right)^k} - r_2^m e^{\frac{-C_0}{k}}}, \quad B = \frac{-p r_2^m e^{\frac{-C_0}{k}}}{r_1^m e^{\frac{-C_0}{k} \left(\frac{r_1}{r_2} \right)^k} - r_2^m e^{\frac{-C_0}{k}}}. \quad (13)$$

Putting A and B values from Eq.(13) into Eq.(12), we have

$$T_{rr} = \frac{-p r^m e^{\frac{-C_0}{k} \left(\frac{r}{r_2} \right)^k} + p r_2^m e^{\frac{-C_0}{k}}}{r_1^m e^{\frac{-C_0}{k} \left(\frac{r_1}{r_2} \right)^k} - r_2^m e^{\frac{-C_0}{k}}}, \quad T_{\theta\theta} = \frac{(m+1) \left(-p r^m e^{\frac{-C_0}{k} \left(\frac{r}{r_2} \right)^k} + p r_2^m e^{\frac{-C_0}{k}} \right) - p r^m e^{\frac{-C_0}{k} \left(\frac{r}{r_2} \right)^k} \left(m - C_0 \left(\frac{r}{r_2} \right)^k \right)}{r_1^m e^{\frac{-C_0}{k} \left(\frac{r_1}{r_2} \right)^k} - r_2^m e^{\frac{-C_0}{k}}}. \quad (14)$$

Tresca's yield criterion derived from Eq.(14) at $r = r_1$ is as follows:

$$|T_{rr} - T_{\theta\theta}|_{r=r_1} = Y_1,$$

$$Y_1 = \frac{2m p r_1^m e^{-\frac{C_0}{k} \left(\frac{r_1}{r_2}\right)^k} - p r_2^m e^{-\frac{C_0}{k}} - p C_0 r_1^m \left(\frac{r_1}{r_2}\right)^k e^{-\frac{C_0}{k} \left(\frac{r_1}{r_2}\right)^k}}{r_1^m e^{-\frac{C_0}{k} \left(\frac{r_1}{r_2}\right)^k} - r_2^m e^{-\frac{C_0}{k}}} \quad (15)$$

The effective pressure necessary for disc's initial yielding is indicated from Eq.(15) as

$$\frac{p}{Y_1} = \frac{\left(\frac{r_1}{r_2}\right)^m e^{-\frac{C_0}{k} \left(\frac{r_1}{r_2}\right)^k} - e^{-\frac{C_0}{k}}}{2m \left(\frac{r_1}{r_2}\right)^m e^{-\frac{C_0}{k} \left(\frac{r_1}{r_2}\right)^k} - m e^{-\frac{C_0}{k}} - C_0 \left(\frac{r_1}{r_2}\right)^{m+k} e^{-\frac{C_0}{k} \left(\frac{r_1}{r_2}\right)^k}} \quad (16)$$

Initial yielding appears at the disc's inner surface, and consequently, a completely plastic state appears at the disc's outer surface. As a result, Eq.(15) at $r = r_2$ gives

$$Y_2 = \frac{2m p r_2^m e^{-\frac{C_0}{k}} - m p r_2^m e^{-\frac{C_0}{k}} - p C_0 r_2^m e^{-\frac{C_0}{k}}}{r_1^m e^{-\frac{C_0}{k} \left(\frac{r_1}{r_2}\right)^k} - r_2^m e^{-\frac{C_0}{k}}} \quad (17)$$

For fully plastic state, $C_0 \rightarrow 0$, Eq.(17) becomes

$$Y_2 = \frac{m p r_2^m}{r_1^m - r_2^m} \quad (18)$$

The effective pressure necessary for disc's fully plastic state is indicated from Eq.(18) as

$$\frac{p}{Y_2} = \frac{\left(\frac{r_1}{r_2}\right)^m - 1}{m} \quad (19)$$

We present the subsequent non-dimensional components

$$R = \frac{r}{r_2}; R_0 = \frac{r_1}{r_2}; \sigma_{r1} = \frac{T_{rr}}{Y_1}; \sigma_{\theta 1} = \frac{T_{\theta\theta}}{Y_1}; \sigma_{r2} = \frac{T_{rr}}{Y_2}; \sigma_{\theta 2} = \frac{T_{\theta\theta}}{Y_2}; p_i = \frac{p}{Y_1} \quad (20)$$

Using Eq.(14) and Eq.(20), the transitional stresses in non-dimensional manner can be stated as

$$\sigma_{r1} = \frac{-p_i \left(R^m e^{-\frac{C_0}{k} R^k} - e^{-\frac{C_0}{k}} \right)}{R_0^m e^{-\frac{C_0}{k} R_0^k} - e^{-\frac{C_0}{k}}},$$

$$\sigma_{\theta 1} = \frac{-p_i \left[(m+1) \left(R^m e^{-\frac{C_0}{k} R^k} - e^{-\frac{C_0}{k}} \right) + R^m e^{-\frac{C_0}{k} R^k} (m - C_0 R^k) \right]}{R_0^m e^{-\frac{C_0}{k} R_0^k} - e^{-\frac{C_0}{k}}},$$

$$\sigma_{r2} = \frac{-p_f (R^m - 1)}{R_0^m - 1}, \quad \sigma_{\theta 2} = \frac{-p_f [(m+1)(R^m - 1) + m R^m]}{R_0^k - 1} \quad (21)$$

Non-dimensionally, initial pressure may be described as

$$p_i = \frac{R_0^m e^{-\frac{C_0}{k} R_0^k} - e^{-\frac{C_0}{k}}}{2m R_0^m e^{-\frac{C_0}{k} R_0^k} - m e^{-\frac{C_0}{k}} - C_0 R_0^{m+k} e^{-\frac{C_0}{k} R_0^k}} \quad (22)$$

Non-dimensionally, pressure necessary for fully plastic state can be stated as

$$p_f = \frac{R_0^m - 1}{m} \quad (23)$$

NUMERICAL DISCUSSION

Table 1. Material constants of isotropic materials steel and copper.

Material constant	Steel	Copper
C_0	0.63	0.78

Graphs for transition state

The standard values of all the material constants for the considered materials are used from Table 1

Figure 1 represents the pressure needed for initial yielding in a thin rotating disc for functionally graded isotropic materials (steel and copper) with different values of k and $m = 1.5$. From the graph, it can be seen that for $k = -1$ and $k = -2$, the initial pressure has positive values, but for $k = -3$, the values are negative.

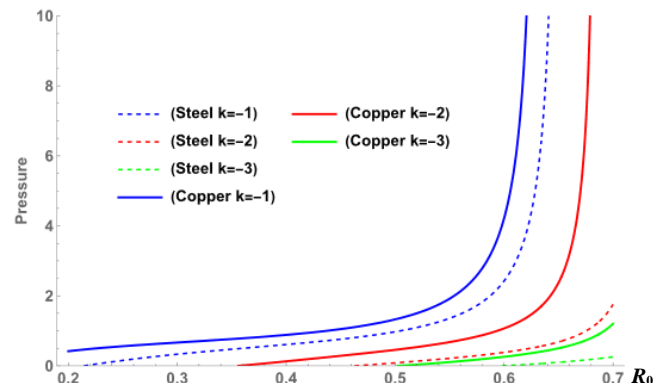


Figure 1. Initial pressure for functionally graded isotropic material (steel and copper) with $m = 1.5$.

Figure 2 represents the pressure needed for initial yielding in a thin rotating disc for functionally graded isotropic materials (steel and copper) with different values of k and $m = 2$. From the graph, it can be seen that for $k = -1$ and $k = -2$, the initial pressure has positive values, but for $k = -3$, the values are negative.

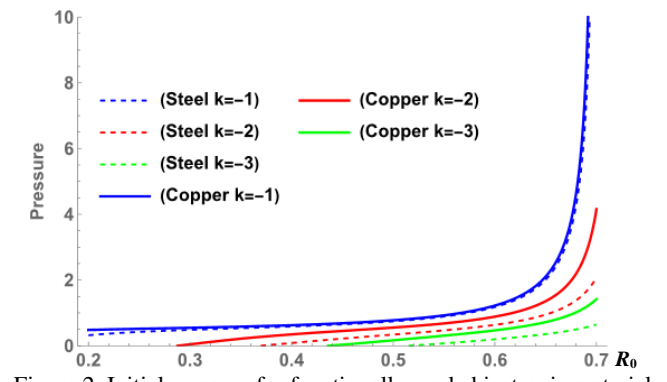


Figure 2. Initial pressure for functionally graded isotropic material (steel and copper) with $m = 2$.

Figure 3 represents the pressure required for initial yielding in a thin rotating disc for functionally graded isotropic materials (steel and copper) with different values of k and $m = 2.5$. From the graph, it can be seen that initial pressure has negative values for $k = -2$ and $k = -3$, but values are positive for $k = -1$ on the inner surface of the disc. For $k = -1$, the values for both materials are approximately the same.

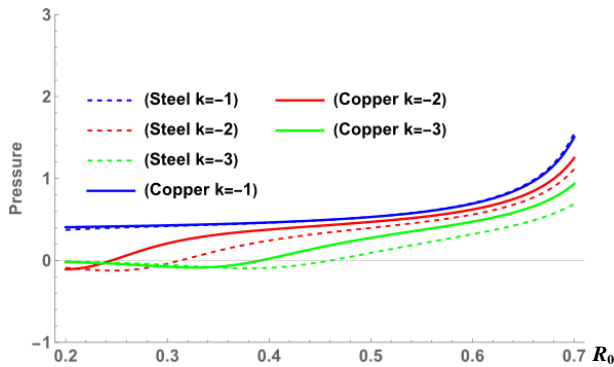


Figure 3. Initial pressure for functionally graded isotropic material (steel and copper) with $m = 2.5$.

From all the Figs. 1-3, it can be seen that if the value of m increases from 1.5 to 2, and then from 2 to 2.5, the values of initial pressure decrease. The initial pressure is minimum on the disc's inner surface and increase as it approaches the outer surface, reaching a maximum at disc's outer surface. It is also seen that values for copper for all three values of k are greater than values for steel for all three values of k .

Figures 4, 5, and 6 represent the circumferential stresses for initial yielding in a thin rotating disc for functionally graded isotropic materials (steel and copper) with different values of k and for $m = 1.5, 2$, and 2.5 , respectively. From all the Figs. 4-6, it can be seen that if m increases from 1.5 to 2, and then from 2 to 2.5, the stresses are more compressive than tensile on the disc's inner surface. Also, the values of circumferential stresses are negative on the disc's inner surface and start increasing towards the outer surface and attain positive values at the disc's outer surface. This implies that the stresses are compressive on the inside and tensile on the disc's outside surface. It is also seen that the stresses for copper for all three values of k are greater than values for steel, for all three values of k .

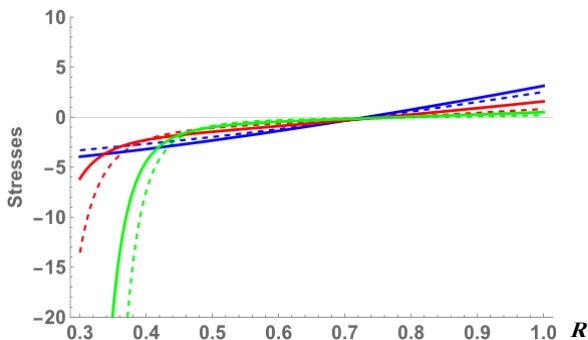
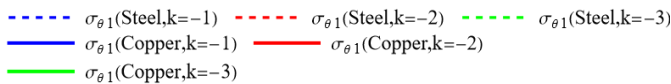


Figure 4. Circumferential stresses for functionally graded isotropic material (steel and copper) with $m = 1.5$.

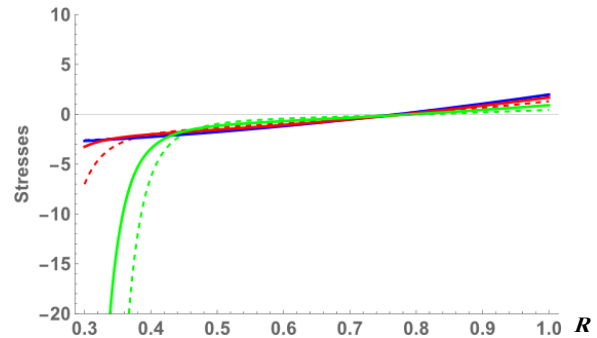


Figure 5. Circumferential stresses for functionally graded isotropic material (steel and copper) with $m = 2$.

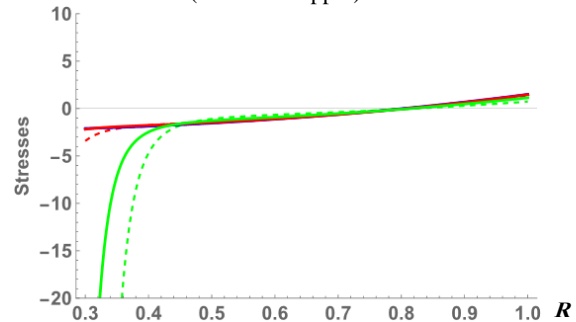


Figure 6. Circumferential stresses for functionally graded isotropic material (steel and copper) with $m = 2.5$.

Graphs for fully plastic state

Figure 7 represents the pressure needed in fully plastic state for functionally graded isotropic materials (steel and copper) with different values of m . From the graph, it can be seen that for all values of m , the pressure has negative values. The values for pressure are minimum on the disc's inner surface and increase by approaching the outer surface, reaching a maximum at the disc's outer surface.

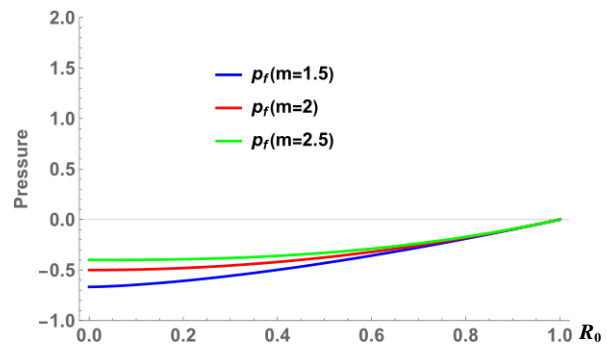


Figure 7. Pressure required fully plastic state for isotropic material (steel and copper) with different values of m .

Figures 8, 9, and 10 represent circumferential stresses for fully plastic state in a thin rotating disc for functionally graded isotropic materials (steel and copper) with different values of k and $m = 1.5, 2$, and 2.5 , respectively. It can be seen that the values of circumferential stresses are positive on the disc's inner surface and decrease as it approaches the outer surface and attain negative values at the disc's outer surface. This implies that stresses are tensile on the inner surface and compressive on the disc's outer surface.

It can also be concluded that as values of m increase, the stresses are tensile on the inner surface and compressive on the disc's outer surface.

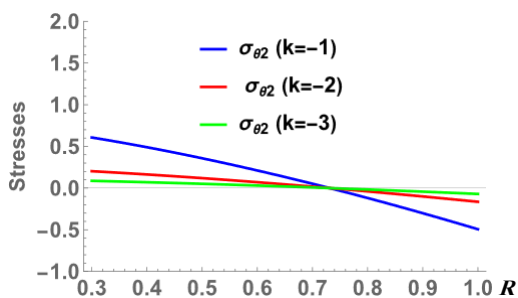


Figure 8. Circumferential stresses for functionally graded isotropic material (steel and copper) with $m = 1.5$.

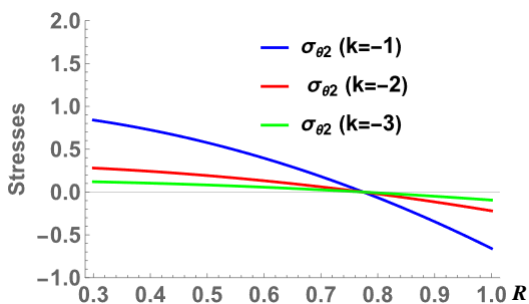


Figure 9. Circumferential stresses for functionally graded isotropic material (steel and copper) with $m = 2$.

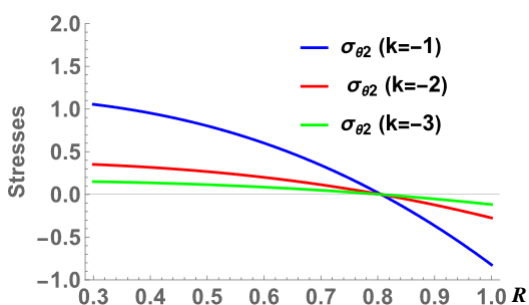


Figure 10. Circumferential stresses for functionally graded isotropic material (steel and copper) with $m = 2.5$.

Particular case (homogeneous isotropic material)

Graphs for transition state

Figure 11 represents the pressure needed for initial yielding in a thin rotating disc for homogeneous isotropic materials (steel and copper) with different values of m . From the graph it can be seen that the values for initial pressure are maximal on the disc's inner surface and decrease by approaching the outer surface and attain minimum value at the disc's outer surface. It can be concluded that values for copper for all three values of m are higher than that of steel.

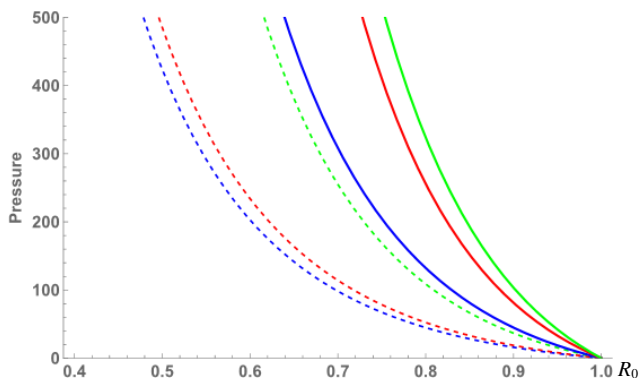


Figure 11. Initial pressure for homogeneous isotropic material (steel and copper) with different values of m .

Figure 12 represents circumferential stresses for initial yielding in a thin rotating disc for homogeneous isotropic materials (steel and copper) with different values of m . From the graph it can be seen that circumferential stresses are maximal on disc's inner surface and start decreasing towards the outer surface and attain minimal value at the disc's outer surface. It can be concluded that values for copper for all three values of m are higher than that of steel.

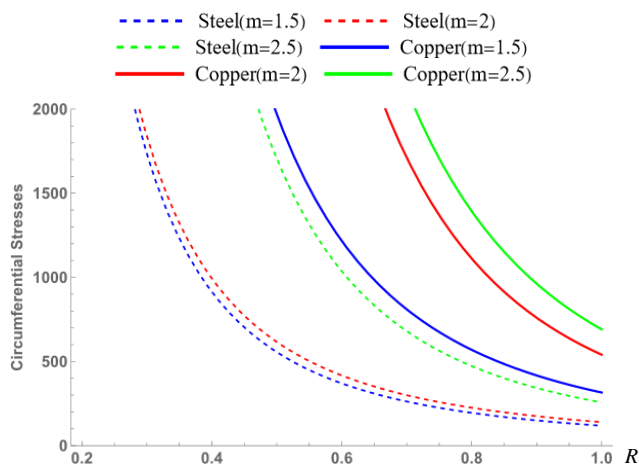


Figure 12. Circumferential stresses for homogeneous isotropic material (steel and copper) with different values of m .

Graphs for fully plastic state

Figure 13 represents the pressure needed for completely plastic state in a thin rotating annular disc of homogeneous isotropic materials (steel and copper) with different values of m . From the graph it can be seen that values for pressure are maximal on disc's inner surface and decrease by approaching disc's outer surface and attain minimal value at disc's outer surface. It can be concluded that the pressure for $m = 2.5$ has a higher value than for other values of m .

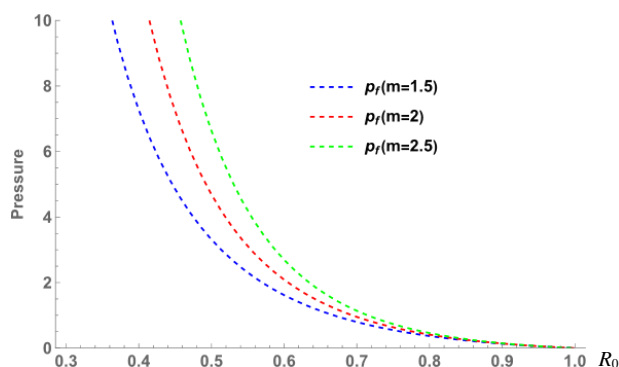


Figure 13. Pressure needed for fully plastic state for homogeneous isotropic material (steel and copper) with different values of m .

Figure 14 represents circumferential stresses for fully plastic state in a disc of homogeneous isotropic materials (steel and copper) with different values of m . From the graph it can be seen that circumferential stresses are highest on disc's inner surface and start decreasing towards the outer surface and attain a minimal value at disc's outer surface. It can be concluded that stresses for $m = 2.5$ have higher value than for other values of m .

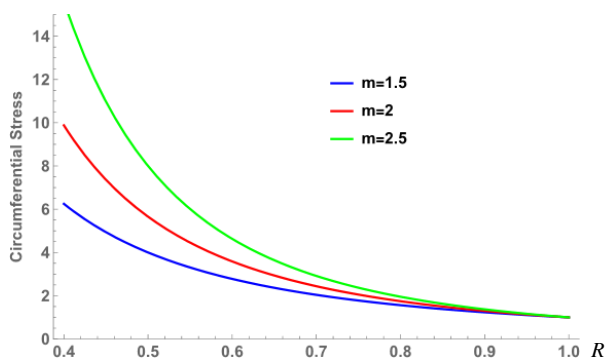


Figure 14. Circumferential stresses for homogeneous isotropic material (steel and copper) with different values of m .

SUMMARY AND CONCLUSION

The analytical solution is acquired for transitional stresses in a very thin spinning disc formed of functionally graded isotropic material having varying compressibility and thickness with internal pressure using mid-zone theory. The previous study results that the annular disc of compressible material needs more pressure at disc's inner surface than the incompressible material's annular disc. When comparing compressible and incompressible materials, the value of hoop stress is greatest at the outer surface of the annular disc of compressible material.

In this study, a comparison between two functionally graded isotropic materials (steel and copper) is done to investigate the effect of variable compressibility and varying thickness on the performance of a thin annular disc in the field of engineering design. Graphs and mathematical computations are used to make the following observations.

The initial pressure for copper for all different values of k has higher values than that of steel.

The circumferential stresses for copper for all three values of k are greater than values for steel for all three values of k .

As value of m increases, the transitional stresses are more compressive than tensile on the disc's inner surface.

Copper with $k = -1$ and $m = 2.5$ has higher circumferential stresses than steel.

Therefore, it can be concluded that the annular disc of FGM (copper) is more suitable for engineering design than the disc formed of steel.

REFERENCES

- Sahni, M., Sahni, R., Patel, N., Kumar, M. (2021), *Frobenius series solution for functionally graded material with exponentially variable thickness and moduli*, Struct. Integr. Life, 21 (Spec. Issue): S83-S88.
- Tan, Y., He, Y., Liu, C., Li, X. (2022), *Phase field fracture model of transversely isotropic piezoelectric materials with thermal effect*, Eng. Fract. Mech. 268: 208479. doi: 10.1016/j.engfrmech.2022.108479
- Mehta, P.D., Sahni, M., Thakur, P. (2019), *Strength analysis of functionally graded rotating disc under variable density and temperature loading*, Struct. Integr. Life, 19: 95-101.
- Nguyen, L.B., Nguyen, N.V., Thai, C.H., et al. (2019), *An isogeometric Bézier finite element analysis for piezoelectric FG porous plates reinforced by graphene platelets*, Compos. Struct. 214: 227-245. doi: 10.1016/j.compstruct.2019.01.077
- Nguyen, N.V., Lee, J., Nguyen-Xuan, H. (2019), *Active vibration control of GPLs-reinforced FG metal foam plates with*

- piezoelectric sensor and actuator layers*, Compos. Part B: Eng. 172: 769-784. doi: 10.1016/j.compositesb.2019.05.060
- Sharma, S., Yadav, S. (2019), *Numerical solution of thermal elastic-plastic functionally graded thin rotating disk with exponentially variable thickness and variable density*, Therm. Sci. 23(1): 125-136. doi: 10.2298/TSCI131001136S
- Shi, P., Xie, J. (2023), *Exact solution of magneto-elastoplastic problem of functionally graded cylinder subjected to internal pressure*, Appl. Math. Model. 123: 835-855. doi: 10.1016/j.apm.2023.08.014
- Khaldi, M., Saeedi, S., Moradi, S.A.Z., et al. (2022), *A successive approximation method for thermo-elasto-plastic analysis of a reinforced functionally graded rotating disc*, Archiv. Civ. Mech. Eng. 22: 2. doi: 10.1007/s43452-021-00321-4
- Bahaloo, H., Nayeab-Hashemi, H. (2022), *Stress analysis and thermoelastic instability of an annular functionally graded rotating disk*, J Therm. Stres. 45(1): 1-11. doi: 10.1080/01495739.2021.2013748
- Bagheri, R., Ayatollahi, M., Mousavi, S.M. (2015), *Analytical solution of multiple moving cracks in functionally graded piezoelectric strip*, Appl. Math. Mech. 36(6): 777-792. doi: 10.1007/s10483-015-1942-6
- Sharma, R., Sahni, M. (2020), *Analysis of creep stresses in thin rotating disc composed of piezoelectric material*, Struct. Integr. Life, Spec. Issue 2020: S47- S49.
- Sharma, S., Yadav, S., Sharma, R. (2017), *Thermal creep analysis of functionally graded thick-walled cylinder subjected to torsion and internal and external pressure*, J Solid Mech. 9 (2): 302-318.
- Sharma, S., Panchal, R. (2017), *Thermal creep deformation in pressurized thick-walled functionally graded rotating spherical shell*, Int. J Pure Appl. Math. 114(3): 435-444. doi: 10.12732/ijpam.v114i3.2
- Sharma, S., Sharma, R., Panchal, R. (2018), *Creep transition in transversely isotropic composite circular cylinder subjected to internal pressure*, Int. J Pure Appl. Math. 120(1): 87-96. doi: 10.12732/ijpam.v120i1.8
- Sharma, S., Yadav, S., Sharma, R. (2018), *Creep torsion in thick-walled circular cylinder under internal and external pressure*, Struct. Integr. Life, 18(2): 89-97.
- Sharma, S., Panchal, R. (2018), *Creep stresses in functionally graded rotating orthotropic cylinder with varying thickness and density under internal and external pressure*, Struct. Integr. Life, 18(2): 111-119.
- Chand, S., Sood, S., Thakur, P., Gupta, K. (2023), *Elasto-plastic stress deformation in an annular disk made of isotropic material and subjected to uniform pressure*, Struct. Integr. Life, 23(1): 61-64.
- Matvienko, O., Daneyko, O., Valikhov, V., et al. (2023), *Elasto-plastic deformation of rotating disk made of aluminum dispersion-hardened alloys*, Metals, 13(6): 1028. doi: 10.3390/met13061028
- Es-Saheb, M.H., Fouad, Y. (2023), *Creep analysis of rotating thick cylinders subjected to external and internal pressure: analytical and numerical approach*, Appl. Sci. 13(21): 11652. doi: 10.3390/app132111652
- Godana, T.A., Singh, S.B., Thakur, P., Kumar, P. (2023), *Modelling the elastoplastic deformation of an internally pressurized transversely isotropic shell under a temperature gradient*, Turk. J Comp. Math. Edu. 14(1): 207-221. doi: 10.17762/turcomat.v14i1.13458

© 2024 The Author. Structural Integrity and Life, Published by DIVK (The Society for Structural Integrity and Life 'Prof. Dr Stojan Sedmak') (<http://divk.inovacionicentar.rs/ivk/home.html>). This is an open access article distributed under the terms and conditions of the Creative Commons Attribution-NonCommercial-NoDerivatives 4.0 International License